

Detecting the Exchange Phase of Majorana Bound States in a Corbino Geometry Topological Josephson Junction

Sunghun Park¹ and Patrik Recher^{1,2}

¹*Institute for Mathematical Physics, TU Braunschweig, D-38106 Braunschweig, Germany*

²*Laboratory for Emerging Nanometrology Braunschweig, D-38106 Braunschweig, Germany*

(Dated: June 16, 2021)

A phase from an adiabatic exchange of Majorana bound states (MBS) reveals their exotic anyonic nature. For detecting this exchange phase, we propose an experimental setup consisting of a Corbino geometry Josephson junction on the surface of a topological insulator, in which two MBS at zero energy can be created and rotated. We find that if a metallic tip is weakly coupled to a point on the junction, the time-averaged differential conductance of the tip-Majorana coupling shows peaks at the tip voltages $eV = \pm(\alpha - 2\pi l)\hbar/T_J$, where $\alpha = \pi/2$ is the exchange phase of the two circulating MBS, T_J is the half rotation time of MBS, and l an integer. This result constitutes a clear experimental signature of Majorana fermion exchange.

PACS numbers: 71.10.Pm, 03.65.Vf, 74.45.+c, 73.23.-b

Majorana fermions are charge-neutral quasiparticles obeying non-Abelian exchange statistics that may be useful for quantum computation [1–7]. Over the past years, they have been predicted to appear in certain condensed matter systems, like topological insulators [2, 8], semiconductors with spin-orbit interactions [9, 10], and magnetic atom chains [11–13], in proximity to s -wave superconductors, and the search for experimental signatures of their unusual features has been intensified. For example, the tunneling conductance between a metallic lead and a Majorana fermion shows a zero-bias peak [14, 15], and signatures for this prediction have been identified in experiments [16–19]. Other schemes, such as interferometry in a Dirac-Majorana converter [20, 21] and a Majorana-mediated Josephson effect [22–28], have also been explored. So far, however, most of the signatures that are predicted or observed are attributed to Majorana features associated with charge neutrality and fermion parity anomaly, and less attention has been paid to find signatures from the exchange statistics, although several schemes to realize exchange or braiding operations have been suggested [8, 29–32].

Exchange statistics of Majorana fermions, which differs from that of fermions or bosons, can provide alternative routes of detection. An adiabatic exchange of two Majorana fermions γ_1 and γ_2 leads to the transformation $\gamma_1 \rightarrow \gamma_2$ and $\gamma_2 \rightarrow -\gamma_1$, resulting in exotic phase factors [7]. In Ref. [33], a long circular topological Josephson junction is considered where the energy spectrum of the junction is found to depend on the exchange phase and fermion parity. Finding further experimental signatures of the exchange phase would be an important task for Majorana fermion detection.

In this work, we propose a transport experiment where the exchange phase of mobile Majorana bound states (MBS) can be identified. The setup consists of a Corbino geometry Josephson junction on the surface of a topological insulator. By solving the Bogoliubov-de Gennes equation, we show that two spatially separated MBS at zero excitation energy appear in the junction—lacking

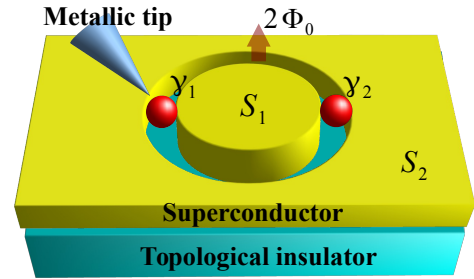


FIG. 1: Schematic of an experimental setup for performing and detecting Majorana exchange. Thin-film superconductors labeled S_1 and S_2 are deposited on the surface of a topological insulator, forming a Corbino-geometry topological Josephson junction. In the presence of two flux quanta [$2\Phi_0$ with $\Phi_0 = h/(2e)$], two zero-energy MBS (red balls denoted by γ_1 and γ_2) appear at opposite sides of the junction. Their positions can be moved slowly while maintaining their relative distance by applying a small voltage across the junction, enabling us to perform an adiabatic exchange. The resulting exchange phase can be identified in the time-averaged differential conductance of a metallic tip weakly tunnel coupled to the junction.

the hybridization between them—when two flux quanta are introduced in the junction. Their positions can be moved along the circle by changing the superconducting phase difference across the junction, allowing for their exchange. If a metallic tip is weakly coupled locally to the junction, and the two MBS are rotating adiabatically, the electron tunneling between the tip and MBS occurs every half rotation period. In this weak coupling limit, we find that the time-averaged differential conductance shows peaks at the tip voltage $eV = \pm(\alpha - 2\pi l)\hbar/T_J$ with $\alpha = \pi/2$ the exchange phase [34]. This provides direct experimental signatures of the nature of Majorana fermion exchange statistics via a dc charge measurement.

Rotating MBS.— We first find MBS in a Corbino geometry Josephson junction deposited on the surface (x - y plane) of a topological insulator. The setup is illustrated

in Fig. 1. The Josephson junction is formed by thin films of inner (S_1) and outer (S_2) s -wave superconductors and contains two magnetic flux quanta. For simplicity, we assume that the distance between S_1 and S_2 is zero. We consider the case where the radius of S_1 denoted by R satisfies $\xi \ll R \ll \Lambda$ so that the vector potential of the magnetic field can be neglected, where ξ is the superconducting coherence length, and Λ is the Pearl length [35]; neglecting the vector potential is justified provided that the flux through the area where the bound states are localized is smaller than the flux quantum [36]. We also assume a short Josephson junction, i.e., $2\pi R \ll \lambda_J$ where λ_J is the Josephson penetration depth [27, 35]. Then the Bogoliubov-de Gennes (BdG) equation with Nambu spinors $\Psi = (\Psi_\uparrow, \Psi_\downarrow, \Psi_\downarrow^\dagger, -\Psi_\uparrow^\dagger)^T$ of excitation energy E has the form [8, 9, 37]

$$\mathcal{H}_{\text{BdG}}\Psi(r, \theta) = E\Psi(r, \theta), \quad (1)$$

$$\mathcal{H}_{\text{BdG}} = \begin{pmatrix} H - \mu & \Delta(r, \theta)\mathbb{I} \\ \Delta^*(r, \theta)\mathbb{I} & \mu - H \end{pmatrix}. \quad (2)$$

Here $H = v_F\vec{\sigma} \cdot \vec{p}$ is the single-particle Hamiltonian describing the surface of the topological insulator, $\vec{\sigma} = (\sigma_x, \sigma_y)$ are Pauli spin matrices, \mathbb{I} is the 2×2 unit matrix, and μ is the chemical potential. The induced gap $\Delta(r, \theta)$ in the presence of the two flux quanta can be described by the position-dependent form as

$$\Delta(r, \theta) = \begin{cases} \Delta_0 e^{i\phi_1} & 0 \leq r < R, \\ \Delta_0 e^{-i2\theta + i\phi_2} & r > R, \end{cases} \quad (3)$$

where ϕ_1 and ϕ_2 are spatially uniform phases in each region, and the polar-angle-dependent term -2θ is due to the flux quanta [35].

We solve Eq. (1) for the case of $\mu = 0$ to obtain Majorana zero-energy states, Ψ_{M1} and Ψ_{M2} , which are spatially separated and orthogonal. They satisfy $\Xi\Psi_{Mj} = \Psi_{Mj}$, $j = 1, 2$ where $\Xi = \sigma_y\tau_y\mathcal{C}$ is the particle-hole operator and \mathcal{C} the operator for complex conjugation. The analytical calculation of the MBS we present in the Supplemental Material [38]. Note that the MBS remain at the zero-energy for nonzero μ (see [38] for the proof). The probability densities of Ψ_{Mj} are shown in Fig. 2 for different values of $\phi_1 - \phi_2$. The result shows that their positions, which are defined by the locations where the probability density takes its maximum, are on opposite sides of the junction's circumference, and vary as a function of $\phi_1 - \phi_2$. We denote the positions by $\theta = \theta_\pm$ with θ_+ (θ_-) for Ψ_{M1} (Ψ_{M2}). They are determined by the condition $\Delta\phi = \pm\pi$ and, thus, can be written as

$$\theta_\pm = \frac{\phi_2 - \phi_1 \pm \pi}{2}, \quad (4)$$

where $\Delta\phi \equiv \phi_1 - \phi_2 + 2\theta$ is the local superconducting phase difference across the junction. It is consistent with the previous studies that Majorana fermions can be found in linear [8, 40] or circular [33] Josephson junction when the (local) difference of the superconducting phase is $\pm\pi$.

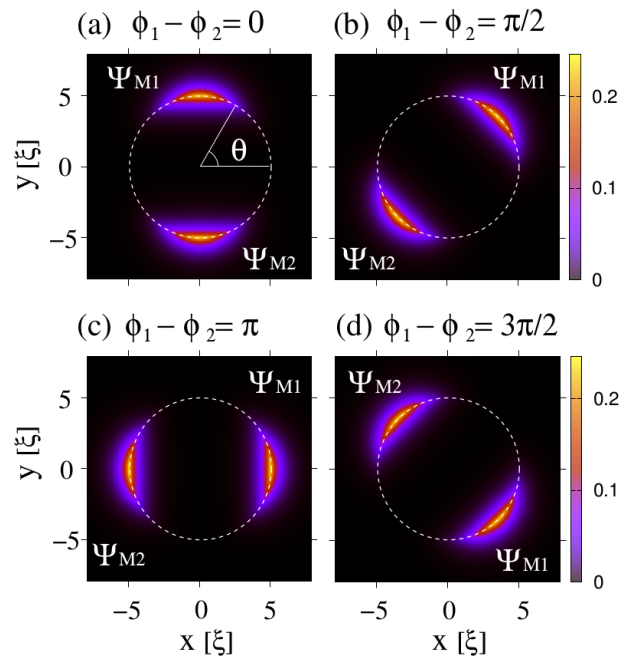


FIG. 2: (a)-(d) Spatial probability densities of the zero-energy MBS, $|\Psi_{M1}|^2$ and $|\Psi_{M2}|^2$, for different values of $\phi_1 - \phi_2$ [see Eq. (4)]. The interface of S_1 and S_2 is depicted by the white dashed circle. The MBS are exchanged (or rotated by π) when $\phi_1 - \phi_2$ varies from 0 to 2π . The parameters are $R = 5\xi$ and $\mu = 0$, where $\xi = \hbar v_F / \Delta_0$ is the superconducting coherence length.

The fact that the positions of the MBS are moved by changing $\phi_1 - \phi_2$ allows us to perform an adiabatic exchange. When we change adiabatically either ϕ_1 from 0 to 2π or ϕ_2 from 0 to -2π , the two MBS rotate by π in a clockwise direction and are exchanged, as shown in Fig. 2. During this operation, they continuously evolve as follows [7]:

$$\Psi_{M1} \rightarrow -s\Psi_{M2}, \quad \Psi_{M2} \rightarrow s\Psi_{M1}, \quad (5)$$

where $s = \pm 1$. $s = 1(-1)$ corresponds to the change of ϕ_1 (ϕ_2) mentioned above. We note that this transformation for the exchange is exact as long as the adiabaticity is fulfilled because the bound states are exactly at zero energy.

The adiabatic change of $\phi_1 - \phi_2$ can be achieved experimentally by applying a constant voltage V_J across the junction. For the adiabaticity, eV_J should be much smaller than the excitation gap to the excited states. Then $\phi_1 - \phi_2$ varies with time t as $\phi_1 - \phi_2 = \phi_0 + 2eV_J t / \hbar$, where ϕ_0 is constant in time. In this case, Ψ_{M1} and Ψ_{M2} become instantaneous zero-energy eigenstates of the time-dependent $\mathcal{H}_{\text{BdG}}[\phi_1(t), \phi_2(t)]$, and their evolution during a half rotation time $T_J = \pi\hbar / (eV_J)$ is described as in Eq. (5) [41]. Equivalently, in terms of Majorana operators, the exchange is expressed as

$$\gamma_1(T_J) = -s\gamma_2(0), \quad \gamma_2(T_J) = s\gamma_1(0). \quad (6)$$

Here, $\gamma_{j=1,2}(t) = \int d^2r \Psi_{M_j}^\dagger(\vec{r}, t)\Phi(\vec{r})$ and $\Phi(\vec{r}) = (\Phi_\uparrow, \Phi_\downarrow, \Phi_\downarrow^\dagger, -\Phi_\uparrow^\dagger)^T$ is the four-component field operator.

Exchange phase and transport.— We now consider a normal metallic tip (STM) tunnel coupled to a position of the Corbino Josephson junction containing two circulating MBS. In this situation, the coupling between the tip and one Majorana state becomes significant or suppressed as the Majorana state approaches to or leaves from the tip, respectively, while the other Majorana state is on the opposite side of the junction with an exponentially small coupling to the tip, leading to occurrence of time-dependent tunneling periodically with period T_J . In each period, MBS are exchanged. We will see below how the resulting exchange phase influences the tunneling differential conductance in this setup.

We perform our calculation in the weak tunneling limit. Also, in order to focus on the low-energy regime where the tip-Majorana coupling dominates, we assume that the voltage $eV_J (= \pi\hbar/T_J)$ across the junction and tip voltage eV are much smaller than the excitation gap.

Then the low-energy Hamiltonian of our setup is

$$H(t) = H_N + H_{\text{BaG}}(t) + H_T(t). \quad (7)$$

$H_N = \sum_{k,\sigma} \varepsilon_k c_{k\sigma}^\dagger c_{k\sigma}$ describes the normal metallic tip where k, σ represent momentum and spin, respectively, and $H_{\text{BaG}}(t) = \frac{1}{2} \int d\vec{r} \Phi^\dagger(\vec{r}) \mathcal{H}_{\text{BaG}}(t) \Phi(\vec{r})$. The tunneling Hamiltonian between the tip and the junction is

$$H_T = \sum_{k,\sigma} \int d^2r [t_{k\sigma}(\vec{r}) c_{k\sigma}^\dagger \Phi_\sigma(\vec{r}) + \text{H.c.}]. \quad (8)$$

As we are interested in low energies, we project H_T onto this low-energy subspace by using $\Phi_\sigma(\vec{r}) = \sum_j \Psi_{j,\sigma}(\vec{r}, t) \gamma_j(t)$. Then we obtain the time-dependent tunneling Hamiltonian,

$$H_T(t) = \sum_{j,k,\sigma} [V_{j,k\sigma}(t) c_{k\sigma}^\dagger \gamma_j(t) + \text{H.c.}], \quad (9)$$

where $V_{j,k\sigma}(t)$ is the coupling coefficient between the tip and $\gamma_j(t)$ at time t , given by

$$V_{j,k\sigma}(t) = \int d^2r t_{k\sigma}(\vec{r}) \Psi_{j,\sigma}(\vec{r}, t). \quad (10)$$

For further development, we consider a specific model for $H_T(t)$. We first define the time sequence $t_q = t_0 + qT_J$ of the coupling with an integer q such that if q is even (odd), $V_{1,k\sigma}(t_q)$ [$V_{2,k\sigma}(t_q)$] is maximal, corresponding to a situation where $\gamma_1(t_q)$ [$\gamma_2(t_q)$] is located closest to the tip, while $\gamma_2(t_q)$ [$\gamma_1(t_q)$] is on the opposite side of the junction with an exponentially small coupling to the tip. Moreover, since MBS are spin polarized, we can restrict the consideration to electrons of one spin species of the tip and, thus, effectively deal with spinless electrons. By taking nearest-neighbor couplings and writing them in terms of $V_{1,k\sigma}(t_0)$ and $\gamma_1(t_0)$ using Eqs. (5) and (6), we obtain the tunneling Hamiltonian at $t = t_q$ as

$$H_T(t_q) = H_T(t_0) = \sum_k [V_k c_k^\dagger \gamma_1(t_0) + \text{H.c.}], \quad (11)$$

where $V_k = V_{1,k\sigma}(t_0)$. Next, around $t = t_q$, we assume that the magnitude of the coupling coefficient varies with time in an exponential manner, while the phase of the coupling does not change significantly; the former assumption is justified by the fact that the MBS show in Fig. 2 are exponentially localized in the azimuthal direction [38], and the latter one is a good approximation provided that $\lambda^{-1} \ll T_J$, where λ^{-1} is the tunneling duration. Then we have

$$H_T(t) = \sum_{q,k} e^{-\lambda|t-t_q|} [V_k c_k^\dagger \gamma_1(t_0) + \text{H.c.}]. \quad (12)$$

The current through the tip is $\langle I(t) \rangle = -e \langle dN_T(t)/dt \rangle$. $N_T(t) = \sum_k c_k^\dagger(t) c_k(t)$ is the tip number operator in the Heisenberg picture with respect to $H(t)$. The expectation value $\langle \cdot \rangle$ is taken over a thermal ensemble of initial states at time $t = t_0$ being in the far past with $H_T = 0$. We switch on H_T at this time [42]. Since tunneling is assumed to be weak, we approximate the time evolution operator of $H(t)$ up to first order in $H_T(t)$ in the interaction picture. We then obtain the tunneling current

$$\begin{aligned} \langle I(t) \rangle &= \frac{1}{i\hbar} \int_{t_0}^t dt' \langle [\hat{I}(t), \hat{H}_T(t')] \rangle \\ &= \frac{2e}{\hbar^2} \text{Re} \left\{ \int_{t_0}^t dt' \sum_{k,q,q'} \Gamma_{k,qq'}(t, t') \right. \\ &\quad \left. \times [G_k(t, t') - \bar{G}_k(t, t')] M(t, t') \right\}, \quad (13) \end{aligned}$$

in the limit of $\lambda^{-1} \ll T_J$, where the operator notation \hat{O} means an interaction picture operator. The current operator is given as

$$\hat{I}(t) = \frac{e}{\hbar} \sum_{q,k} e^{-\lambda|t-t_q|} [iV_k \hat{c}_k^\dagger(t) \hat{\gamma}_1(t) + \text{H.c.}]. \quad (14)$$

We note that $\hat{c}_k^\dagger(t)$ and $\hat{\gamma}_1(t)$ evolve in time under H_N and $H_{\text{BaG}}(t)$, respectively. The tunneling magnitude is defined as

$$\Gamma_{k,qq'}(t, t') = |V_k|^2 e^{-\lambda|t-t_q|} e^{-\lambda|t'-t_{q'}|}. \quad (15)$$

$G_k(t, t')$ and $\bar{G}_k(t, t')$ are the tip electron Green's functions [43], and $M(t, t')$ is the Majorana Green's function

$$M(t, t') = -i \langle \hat{\gamma}_1(t) \hat{\gamma}_1(t') \rangle. \quad (16)$$

This function has the information of the Majorana exchange that is crucial in our proposal. Since the tunneling current is exponentially small except for $t = t_q$ and $t' = t_{q'}$ due to $\Gamma_{k,qq'}(t, t')$, we can approximate $M(t, t') = M(t_q, t_{q'}) = -i \langle \hat{\gamma}_1(t_q) \hat{\gamma}_1(t_{q'}) \rangle$. In the adiabatic limit, the time evolution operator satisfying $\hat{\gamma}_1(t + T_J) = U_M^\dagger \hat{\gamma}_1(t) U_M$ is [7]

$$U_M = \exp \left[\frac{\alpha}{2} \gamma_2(t_0) \gamma_1(t_0) \right], \quad (17)$$

where $\alpha = s\pi/2$ is the exchange phase where $s = \pm 1$ was defined in Eq. (6). From the transformations $\hat{\gamma}_1(t_{q(\nu)}) = [U_M^\dagger]^{q(\nu)} \gamma_1(t_0) [U_M]^{q(\nu)}$, $M(t_q, t_{q'})$ can be obtained as

$$\begin{aligned} M(t_q, t_{q'}) &= -\frac{i}{2} \left\{ [e^{i\alpha(q-q')} + e^{-i\alpha(q-q')}] \right. \\ &\quad \left. + \mathcal{P}(t_0) [e^{i\alpha(q-q')} - e^{-i\alpha(q-q')}] \right\} \\ &\equiv -ie^{i\eta\alpha(q-q')}. \end{aligned} \quad (18)$$

Here, $\mathcal{P}(t_0) = -i\langle \gamma_1(t_0)\gamma_2(t_0) \rangle$ is the fermion parity of the junction at $t = t_0$ and is equal to 1(-1) when the two MBS share no (one) fermion, and $\eta = \pm 1$ for $\mathcal{P}(t_0) = \pm 1$. By substituting Eq. (18) into Eq. (13), we can obtain the tunneling current $\langle I(t) \rangle$ as a function of time t and the tip voltage eV .

We discuss the voltage dependence of the time-averaged differential conductance $d\bar{I}/dV$ [38]. It is enough to consider the current for $\alpha = \pi/2$ and $\eta = 1$ as it is the same for α and η with opposite signs. In the limit of $\lambda^{-1} \ll T_J$, we obtain

$$\frac{d\bar{I}}{dV} = \frac{e^2}{h} \sum_l \frac{Z_l(\alpha)}{4k_B T} \left\{ \operatorname{sech}^2 \left[\frac{V_l^-(\alpha)}{2k_B T} \right] + \operatorname{sech}^2 \left[\frac{V_l^+(\alpha)}{2k_B T} \right] \right\}, \quad (19)$$

where

$$Z_l(\alpha) = 2\pi\Gamma \left[\frac{2\lambda T_J}{\lambda^2 T_J^2 + (\alpha - 2\pi l)^2} \right]^2, \quad (20)$$

and

$$V_l^\pm(\alpha) = \pm eV - \frac{\hbar}{T_J}(\alpha - 2\pi l), \quad (21)$$

with $l = 0, \pm 1, \pm 2, \dots$. Here, $\Gamma = 2\pi\rho|V_k|^2$ is the tunneling energy, and ρ is the tip density of states at the Fermi level. We assume the wide-band limit for the tip so that Γ becomes energy independent. The calculated $d\bar{I}/dV$ is valid for $k_B T \gg |Z_0(\alpha)|$. It shows peaks at $eV = \pm(\alpha - 2\pi l)\hbar/T_J$ with height $(e^2/h)Z_l(\alpha)/(4k_B T)$ as shown in Fig. 3.

Discussion and experimental feasibility.— We have shown that the time-averaged differential conductance between the metallic tip and the Corbino-Josephson junction hosting two rotating MBS exhibits peaks at $eV = \pm(\alpha - 2\pi l)\hbar/T_J$, regardless of the fermion parity of the junction. This feature results from the coherent interference in the time-dependent tip-Majorana tunneling where the exchange phase α from the half rotation of MBS introduces a relative phase between the tunneling at time t' and $t' + T_J$, as shown in Eq. (18). We emphasize that, different from the case of tunneling between the tip and a static MBS which yields a zero voltage conductance peak [15], we have conductance peaks at *nonzero voltage* for *zero-energy* MBS due to the exchange operation. The height of the conductance peaks decreases with increasing tip voltage. This is because when the voltage

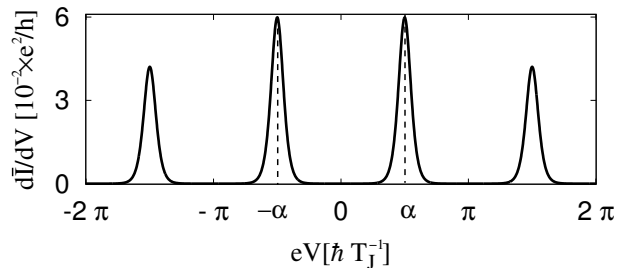


FIG. 3: Time-averaged differential conductance as a function of eV . The parameters are $\hbar T_J^{-1} = 0.1 \text{ meV} = 10^{-1} \hbar\lambda = 10k_B T = 10\Gamma$. The exchange phase $\alpha = \pi/2$ is used. Around zero voltage, the peaks emerge at $eV = \pm\alpha\hbar T_J^{-1}$.

increases, the correlation time of electrons in the metallic tip $\hbar/(eV)$ becomes much smaller than T_J , leading to the suppression of the interference between tunneling at t' and $t' + T_J$ and, hence, to a decreasing peak height. We note that the position of the conductance peaks can also be understood by considering an effective Floquet Hamiltonian as the BdG Hamiltonian is periodic in time with period T_J [38].

We now discuss the experimental feasibility. In our proposal, we require thin-film superconductors whose Pearl length Λ is much larger than the values of R and ξ . Thin-film NbN superconductors have $\Lambda \sim 30 \mu\text{m}$, $\xi \sim 3.5 \text{ nm}$, and superconducting gap $\Delta_{\text{SC}} \sim 3 \text{ meV}$ [44]. Assuming the proximity-induced gap $\Delta_0 \sim 1 \text{ meV}$, the excitation gap of our Corbino-Josephson junction can be estimated by $E_g \sim \sqrt{2\Delta_0\hbar v_F}/R \sim 0.63 \text{ meV}$ for $R = 5\hbar v_F/\Delta_0$ and $\mu = 0$, where $\tilde{v}_F = v_F\Delta_0^2/(\mu^2 + \Delta_0^2)$ [8]. Next, in order to have adiabatic rotation of the MBS and a short tunneling duration, T_J should be long so that $\hbar/T_J (= eV_J/\pi) \ll \min\{\hbar\lambda, E_g\}$, but sufficiently short so that $T_J \ll t_{QP}$ where t_{QP} is the quasiparticle poisoning time that is in the range of 0.1–1 μs [45]. Estimating $\min\{\hbar\lambda, E_g\} \sim 0.63 \text{ meV}$ and $\hbar/t_{QP} \sim 6.6 \text{ neV}$, gives $\hbar/T_J \sim 10^2 \mu\text{eV}$ for adiabatic interference without quasiparticle poisoning. In order to observe clearly the conductance peaks shown in Fig. 3, the temperature should be smaller than \hbar/T_J which provides an experimentally feasible temperature range of 10–10² mK. We finally note that the MBS are robust against weak disorder; i.e., they remain at zero energy [38], and, hence, the disorder has no significant effect on our results in Fig. 3.

In conclusion, we have proposed an experimental setup where the exchange phase of mobile MBS can be probed as a result of their interference effect. Different from the preceding detection schemes relying on charge neutrality of zero-energy MBS, our setup allows us to identify the nontrivial MBS statistics, providing alternative routes of MBS detection.

We thank C. W. J. Beenakker, F. Pientka, H.-S. Sim, B. Trauzettel, B. van Heck, and L. Weithofer for valuable discussions. P.R. acknowledges financial support from the EU-FP7 Project SE2ND No. 271554 and the DFG

-
- [1] A. Y. Kitaev, Phys. Usp. **44**, 131 (2001).
- [2] M. Z. Hasan and C. L. Kane, Rev. Mod. Phys. **82**, 3045 (2010).
- [3] J. Alicea, Rep. Prog. Phys. **75**, 076501 (2012).
- [4] C. W. J. Beenakker, Annu. Rev. Condens. Matter Phys. **4**, 113 (2013).
- [5] C. Nayak, S. H. Simon, A. Stern, M. Freedman, and S. Das Sarma, Rev. Mod. Phys. **80**, 1083 (2008).
- [6] G. Moore and N. Read, Nucl. Phys. **B360**, 362 (1991).
- [7] D. A. Ivanov, Phys. Rev. Lett **86**, 268 (2001).
- [8] L. Fu and C. L. Kane, Phys. Rev. Lett **100**, 096407 (2008).
- [9] J. D. Sau, R. M. Lutchyn, S. Tewari, and S. Das Sarma, Phys. Rev. Lett **104**, 040502 (2010).
- [10] Y. Oreg, G. Refael, and F. von Oppen, Phys. Rev. Lett. **105**, 177002 (2010).
- [11] T.-P. Choy, J. M. Edge, A. R. Akhmerov, and C. W. J. Beenakker, Phys. Rev. B **84**, 195442 (2011).
- [12] S. Nadj-Perge, I. K. Drozdov, B. A. Bernevig, and A. Yazdani, Phys. Rev. B **88**, 020407(R) (2013).
- [13] S. Nadj-Perge, I. K. Drozdov, J. Li, H. Chen, S. Jeon, J. Seo, A. H. MacDonald, B. A. Bernevig, and A. Yazdani, Science **346**, 602 (2014).
- [14] K. T. Law, P. A. Lee, and T. K. Ng, Phys. Rev. Lett. **103**, 237001 (2009).
- [15] K. Flensberg, Phys. Rev. B **82**, 180516(R) (2010).
- [16] V. Mourik, K. Zuo, S. M. Frolov, S. R. Plissard, E. P. A. M. Bakkers, and L. P. Kouwenhoven, Science **336**, 1003 (2012).
- [17] A. Das, Y. Ronen, Y. Most, Y. Oreg, M. Heiblum, and H. Shtrikman, Nat. Phys. **8**, 887 (2012).
- [18] M.T. Deng, C.L. Yu, G.Y. Huang, M. Larsson, P. Caroff, and H.Q. Xu, Nano Lett. **12**, 6414 (2012).
- [19] E. J. H. Lee, X. Jiang, M. Houzet, R. Aguado, C. M. Lieber, and S. De Franceschi, Nat. Nanotechnol. **9**, 79 (2014).
- [20] L. Fu and C. L. Kane, Phys. Rev. Lett. **102**, 216403 (2009).
- [21] A. R. Akhmerov, J. Nilsson, and C. W. J. Beenakker, Phys. Rev. Lett. **102**, 216404 (2009).
- [22] L. Fu and C. L. Kane, Phys. Rev. B **79**, 161408(R) (2009).
- [23] P. A. Ioselevich and M. V. Feigel'man, Phys. Rev. Lett. **106**, 077003 (2011).
- [24] L. Jiang, D. Pekker, J. Alicea, G. Refael, Y. Oreg, and F. von Oppen, Phys. Rev. Lett. **107**, 236401 (2011).
- [25] L. P. Rokhinson, X. Liu, and J. K. Furdyna, Nat. Phys. **8**, 795 (2012).
- [26] B. Sacépé, J. B. Oostinga, J. Li, A. Ubaldini, N. J. G. Couto, E. Giannini, and A. F. Morpurgo, Nat. Commun. **2**, 575 (2011).
- [27] J. R. Williams, A. J. Bestwick, P. Gallagher, S. S. Hong, Y. Cui, A. S. Bleich, J. G. Analytis, I. R. Fisher, and D. Goldhaber-Gordon, Phys. Rev. Lett. **109**, 056803 (2012).
- [28] M. Veldhorst, M. Snelder, M. Hoek, T. Gang, V. K. Guduru, X. L. Wang, U. Zeitler, W. G. van der Wiel, A. A. Golubov, H. Hilgenkamp, and A. Brinkman, Nat. Mater. **11**, 417 (2012).
- [29] J. Alicea, Y. Oreg, G. Refael, F. von Oppen, and M. P. A. Fisher, Nat. Phys. **7**, 412 (2011).
- [30] B. van Heck, A. R. Akhmerov, F. Hassler, M. Burrello, and C. W. J. Beenakker, New J. Phys. **14**, 035019 (2012).
- [31] J. Li, T. Neupert, B. A. Bernevig, and A. Yazdani, arXiv:1404.4058.
- [32] T. Karzig, F. Pientka, G. Refael, and F. von Oppen, Phys. Rev. B **91**, 201102(R) (2015).
- [33] E. Grosfeld and A. Stern, Proc. Natl. Acad. Sci. U.S.A. **108**, 11810 (2011).
- [34] Although Majorana exchange in a system of two MBS γ_1 and γ_2 cannot change the occupation of the non-local fermion $f = (\gamma_1 + i\gamma_2)/2$ in Ref. [7], our tunneling setup shown in Fig. 1 detects the exchange phase of two MBS via an interference effect between different orders of exchange (or braiding) cycles.
- [35] J. R. Clem, Phys. Rev. B **82**, 174515 (2010).
- [36] R. S. Akzyanov, A. V. Rozhkov, A. L. Rakhmanov, and F. Nori, Phys. Rev. B **89**, 085409 (2014).
- [37] A. L. Rakhmanov, A. V. Rozhkov, and F. Nori, Phys. Rev. B **84**, 075141 (2011).
- [38] See the Supplemental Material, which includes Refs. [8, 39], for further details on the derivation of MBS, the calculation of \bar{I} , and the effect of weak disorder.
- [39] J. Cayssol, B. Dóra, F. Simon, and R. Moessner, Phys. Status Solidi RRL **7**, 101 (2013).
- [40] A. C. Potter and L. Fu, Phys. Rev. B **88**, 121109(R) (2013).
- [41] Note that $\mathcal{H}_{\text{BDG}}(\phi_1(t), \phi_2(t))$ is periodic in time with periodicity T_J if either ϕ_1 or ϕ_2 is changed in time.
- [42] Different switching-on times give the same current as long as they are far away from t (by many exchange periods T_J).
- [43] The tip electron Green's functions are given by $iG_k(t, t') = \langle \hat{c}_k(t) \hat{c}_k^\dagger(t') \rangle = e^{-i(\varepsilon_k + eV)(t-t')/\hbar} [1 - n_F(\varepsilon_k)]$, and $i\bar{G}_k(t, t') = \langle \hat{c}_k^\dagger(t) \hat{c}_k(t') \rangle = e^{i(\varepsilon_k + eV)(t-t')/\hbar} n_F(\varepsilon_k)$ where $n_F(\varepsilon_k) = 1/[1 + e^{\varepsilon_k/(k_B T)}]$ is the Fermi-Dirac distribution at $t = t_0$, and tip voltage V .
- [44] S.-Z. Lin, O. Ayala-Valenzuela, R. D. McDonald, L. N. Bulaevskii, T. G. Holesinger, F. Ronning, N. R. Weisse-Bernstein, T. L. Williamson, A. H. Mueller, M. A. Hoffbauer, M. W. Rabin, and M. J. Graf, Phys. Rev. B **87**, 184507 (2013).
- [45] D. Rainis and D. Loss, Phys. Rev. B **85**, 174533 (2012).

Supplemental material for “Detecting the Exchange Phase of Majorana Bound States in a Corbino Geometry Topological Josephson Junction”

Sunghun Park¹ and Patrik Recher^{1,2}

¹*Institute for Mathematical Physics, TU Braunschweig, 38106 Braunschweig, Germany*

²*Laboratory for Emerging Nanometrology Braunschweig, D-38106 Braunschweig, Germany*

In this Supplementary Material, we analytically derive Majorana zero-energy states for $\mu = 0$ and prove that they are still at zero energy for finite μ . Next, we provide the details of the calculation of the time-averaged tunneling current \bar{I} in the main text, and an alternative explanation for the result shown in Fig. 3 using Floquet theory. Finally, we discuss disorder effects.

A. Derivation of Majorana zero energy states

In this section, we first calculate Majorana zero-energy states, Ψ_{M1} and Ψ_{M2} , for $\mu = 0$ by solving the BdG equation for the Corbino geometry. From Eqs. (1) and (2) in the main text, the BdG equation for $\mu = 0$ is given by

$$\begin{pmatrix} v_F \vec{\sigma} \cdot \vec{p} & \Delta(r, \theta) \mathbb{I} \\ \Delta^*(r, \theta) \mathbb{I} & -v_F \vec{\sigma} \cdot \vec{p} \end{pmatrix} \Psi(r, \theta) = E \Psi(r, \theta). \quad (22)$$

This decouples into two sets of equations, one for spin up and one for spin down. We consider only the equations with spin down as those for spin up give diverging solutions which are not physical. Due to the absence of rotation symmetry of the system, the wave function in each region should be given in the form of a superposition of different angular momentum eigenstates. Hereafter we will measure energy and length in units of gap magnitude Δ_0 and superconducting coherence length $\xi = \hbar v_F / \Delta_0$, respectively. With these units, the wave function for the region of $0 \leq r < R$ is expressed as

$$\Psi^<(r, \theta) = \sum_{m=-\infty}^{\infty} a_m \Psi_m^<(r, \theta). \quad (23)$$

Here, a_m are coefficients to be determined below, and $\Psi_m^<(r, \theta)$ is defined as

$$\Psi_m^<(r, \theta) = \begin{pmatrix} 0 \\ e^{i(m+1)\theta} e^{i\phi_1/2} J_{m+1}(ir) \\ -e^{im\theta} e^{-i\phi_1/2} J_m(ir) \\ 0 \end{pmatrix}, \quad (24)$$

where $J_m(ir)$ is the Bessel function of the first kind that is regular at the origin $r = 0$. For $r > R$, the wave function is found as

$$\Psi^>(r, \theta) = \sum_{n=-\infty}^{\infty} b_n \Psi_n^>(r, \theta), \quad (25)$$

with coefficients b_n , and

$$\Psi_n^>(r, \theta) = \begin{pmatrix} 0 \\ e^{in\theta} e^{i\phi_2/2} r H_{n+1}^{(1)}(ir) \\ -e^{i(n+1)\theta} e^{-i\phi_2/2} r H_n^{(1)}(ir) \\ 0 \end{pmatrix}, \quad (26)$$

with $H_n^{(1)}(ir)$ the Hankel function of the first kind that goes to zero as $r \rightarrow \infty$. In order to obtain solutions, we determine the coefficients a_m and b_n by matching the wave functions $\Psi^<(r, \theta)$ and $\Psi^>(r, \theta)$ at $r = R$, leading to

$$\begin{aligned} a_l e^{i\phi_1/2} J_{l+1}(iR) &= b_{l+1} e^{i\phi_2/2} R H_{l+2}(iR), \\ a_{l+1} e^{-i\phi_1/2} J_{l+1}(iR) &= b_l e^{-i\phi_2/2} R H_l(iR), \end{aligned} \quad (27)$$

and the following recurrence relations can be derived,

$$\begin{aligned} a_{l+2} &= e^{i(\phi_1 - \phi_2)} \frac{H_{l+1}(iR)J_{l+1}(iR)}{H_{l+2}(iR)J_{l+2}(iR)} a_l, \\ b_{l'+2} &= e^{i(\phi_1 - \phi_2)} \frac{H_{l'}(iR)J_{l'+2}(iR)}{H_{l'+3}(iR)J_{l'+1}(iR)} b_{l'}, \end{aligned} \quad (28)$$

where l and l' range over all integers. Eqs. (27) and (28) allow us to express the coefficients $a_{l=\text{even}}$ and $b_{l'=\text{odd}}$ ($a_{l=\text{odd}}$ and $b_{l'=\text{even}}$) in terms of a_0 (a_{-1}). This fact indicates that we can construct two independent solutions, denoted by Ψ_1 and Ψ_2 ,

$$\begin{aligned} \Psi_1 &= \Theta(R-r) \sum_{m=\text{even}} a_m \Psi_m^< + \Theta(r-R) \sum_{n=\text{odd}} b_n \Psi_n^>, \\ \Psi_2 &= \Theta(R-r) \sum_{m=\text{odd}} a_m \Psi_m^< + \Theta(r-R) \sum_{n=\text{even}} b_n \Psi_n^>, \end{aligned} \quad (29)$$

with one unknown coefficient a_0 (a_{-1}) for Ψ_1 (Ψ_2), where $\Theta(x)$ is the unit step function. According to the particle-hole symmetry, if Ψ_1 is a solution, then $\Xi\Psi_1$ is also a solution, where $\Xi = \sigma_y \tau_y \mathcal{C}$ is the particle-hole operator with \mathcal{C} the operator of complex conjugation. This imposes a constraint $\Psi_2 = \Xi\Psi_1$, and hence $a_{-1} = -a_0^*$. We choose $a_0 = e^{i(\phi_1 - \phi_2)/4}/\sqrt{N}$ and $a_{-1} = -e^{-i(\phi_1 - \phi_2)/4}/\sqrt{N}$ where N is the normalization constant. The following combinations of Ψ_1 and Ψ_2 give two MBS,

$$\Psi_{M1} = \frac{1}{\sqrt{2}}(\Psi_1 + \Psi_2), \quad \Psi_{M2} = \frac{i}{\sqrt{2}}(\Psi_1 - \Psi_2), \quad (30)$$

which are plotted in Fig. 2 in the main text.

We show that Ψ_{M1} and Ψ_{M2} , centered at $\theta = \theta_{\pm}$, respectively, are exponentially localized in the azimuthal direction to justify the assumption in Eq. (12) in the main text that the coupling between the tip and MBS is exponentially small except for $t = t_q$ where $t_q = t_0 + qT_J$ with an integer q . We first solve an effective low-energy Hamiltonian which is the $k \cdot p$ Hamiltonian obtained by Fu and Kane in Ref. [S1] incorporating the spatial variation of a superconducting phase difference due to two flux quanta in the Josephson junction,

$$\mathcal{H}_{\text{eff}} = \begin{pmatrix} -i\frac{\hbar\tilde{v}}{R}\partial_{\theta} & -i\Delta_0\cos\left(\frac{\Delta\phi}{2}\right) \\ i\Delta_0\cos\left(\frac{\Delta\phi}{2}\right) & i\frac{\hbar\tilde{v}}{R}\partial_{\theta} \end{pmatrix}, \quad (31)$$

where $\tilde{v} = v_F[\cos(\mu W/\hbar v_F) + (\Delta_0/\mu)\sin(\mu W/\hbar v_F)]\Delta_0^2/(\mu^2 + \Delta_0^2)$, μ is the chemical potential, W is the distance between two superconductors, and $\Delta\phi = \phi_1 - \phi_2 + 2\theta$ is the phase difference of the Josephson junction. The effective Hamiltonian, whose bases are two branches of counter-propagating helical Majorana states after integrating out the transverse (radial) degree of freedom, is a good approximation in the limit of $R \gg \xi'$ where $\xi' = \hbar\tilde{v}/\Delta_0$. To calculate approximate zero energy solutions localized at $\theta = \theta_p$ with $p \in \{+, -\}$, we linearize $\cos(\Delta\phi/2)$ around $\Delta\phi = p\pi$,

$$\begin{aligned} \cos\left(\frac{\Delta\phi}{2}\right) &= \cos\left(\frac{p\pi + 2\delta\theta_p}{2}\right) \\ &= -p \sin(\delta\theta_p) \\ &\approx -p \delta\theta_p \end{aligned} \quad (32)$$

for small $\delta\theta_p$ where $\delta\theta_p \equiv \theta - \theta_p$. Then we obtain the exactly solvable Hamiltonian

$$\mathcal{H}_{\text{eff}} = \begin{pmatrix} -i\frac{\hbar\tilde{v}}{R}\partial_{\theta} & -ip\Delta_0\delta\theta_p \\ ip\Delta_0\delta\theta_p & i\frac{\hbar\tilde{v}}{R}\partial_{\theta} \end{pmatrix}, \quad (33)$$

thus allowing us to calculate the zero energy solutions or approximate Majorana states which are exponentially localized in the azimuthal direction, given by

$$\Psi_p^{\text{approx}}(\theta) = \left(\frac{R}{4\pi\xi'}\right)^{1/4} \exp\left[-\frac{R}{2\xi'}(\theta - \theta_p)^2\right] \begin{pmatrix} 1 \\ -p \end{pmatrix}, \quad (34)$$

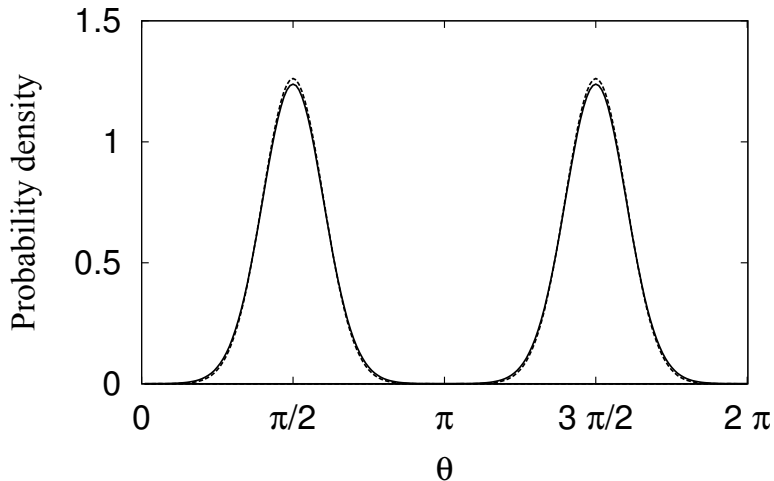


FIG. 4: Probability densities of MBS as a function of azimuthal angle θ for the values of $\theta_{\pm} = \pm\pi/2$, $R = 5\xi'$ and $\mu = W = 0$. Probability densities of $\Psi_{j=M1,M2}^{\text{exact}}(\theta)$ in Eq. (36) are drawn by the solid line, and those of approximate solutions $\Psi_{p=+,-}^{\text{approx}}(\theta)$ in Eq. (35) are drawn by the dashed line.

and probability densities

$$|\Psi_p^{\text{approx}}(\theta)|^2 = \sqrt{\frac{R}{\pi\xi'}} \exp\left[-\frac{R}{\xi'}(\theta - \theta_p)^2\right]. \quad (35)$$

To compare these approximate solutions with the exact MBS given in Eq. (30), we integrate out the radial degrees of freedom of $\Psi_{M1}(r, \theta)$ and $\Psi_{M2}(r, \theta)$,

$$|\Psi_{M1(M2)}^{\text{exact}}(\theta)|^2 = \int dr r |\Psi_{M1(M2)}(r, \theta)|^2. \quad (36)$$

Fig. 4 shows the comparison between $\Psi_{j=M1,M2}^{\text{exact}}(\theta)$ and $\Psi_{p=+,-}^{\text{approx}}(\theta)$, exhibiting a quantitatively good agreement between them. This leads us to the conclusion that MBS found in Eq. (30) are exponentially localized in the azimuthal direction, and hence the form of the tunneling Hamiltonian of Eq. (12) in the main text is a good approximation.

B. Zero-energy Majorana bound states for non-zero chemical potential

We prove that Majorana bound states remain at zero energy for finite μ by using a Taylor expansion around $\mu = 0$. We start the proof by rewriting Eq. (1) in the main text as

$$\mathcal{H}_{\text{BdG}}(\mu)\Psi_j(\mu) = E_j(\mu)\Psi_j(\mu), \quad (37)$$

where $E_{j=1,2}(\mu)$ are the two lowest eigenvalues which are assumed to be differentiable functions with respect to μ , and $\Psi_{j=1,2}(\mu)$ are corresponding eigenstates. In the limit of $\mu \rightarrow 0$, $E_j(\mu) = 0$ and $\Psi_j(\mu)$ become two Majorana bound states, $\Psi_1(0) = \Psi_{M1}$ and $\Psi_2(0) = \Psi_{M2}$. Throughout this section, we use the notation $|\tilde{\Psi}\rangle = \Xi|\Psi\rangle$ as the particle-hole transformed counterpart of $|\Psi\rangle$ where $\Xi = \tau_y\sigma_y\mathcal{C}$ is the particle-hole operator. We note that $\langle\tilde{\Psi}'|\tilde{\Psi}\rangle = \langle\Psi'|\Psi\rangle^*$ by the anti-unitary property of Ξ . And $|\tilde{\Psi}\rangle = |\Psi\rangle$ if $|\Psi\rangle$ is a Majorana state. Below, we will show that $E_j(\mu) = 0$ also for finite μ .

The Taylor expansion of the BdG equation in terms of μ leads to

$$\mathcal{H}_{\text{BdG}}(\mu) = \mathcal{H}_{\text{BdG}}(0) - \mu\tau_z, \quad (38)$$

$$E_j(\mu) = E_{j,0} + E_{j,1}\mu + \frac{1}{2!}E_{j,2}\mu^2 + \frac{1}{3!}E_{j,3}\mu^3 + \dots, \quad (39)$$

$$\Psi_j(\mu) = \Psi_{j,0} + \Psi_{j,1}\mu + \frac{1}{2!}\Psi_{j,2}\mu^2 + \frac{1}{3!}\Psi_{j,3}\mu^3 + \dots, \quad (40)$$

where

$$E_{j,n} \equiv \left. \frac{\partial^n E(\mu)}{\partial \mu^n} \right|_{\mu=0}, \quad \Psi_{j,n} \equiv \left. \frac{\partial^n \Psi_j(\mu)}{\partial \mu^n} \right|_{\mu=0}, \quad (41)$$

and N is the normalization constant. We note that $E_{j,0} = 0$ and $\Psi_{j,0} = \Psi_{Mj}$. By substituting these series into Eq. (37) and equating the terms in each power of μ , we obtain equations for zeroth-order, first-order, and so on, each of which is discussed below.

The equation for the zeroth order of μ is given by

$$\mathcal{H}_{\text{BdG}}(0)\Psi_{j,0} = E_{j,0}\Psi_{j,0} = 0, \quad (42)$$

which is trivial.

Next, we consider the first-order equation given by

$$\mathcal{H}_{\text{BdG}}(0)\Psi_{j,1} - \tau_z \Psi_{j,0} = E_{j,1}\Psi_{j,0}. \quad (43)$$

If we multiply by $\langle \Psi_{j,0} |$, it yields

$$\langle \Psi_{j,0} | \mathcal{H}_{\text{BdG}}(0) | \Psi_{j,1} \rangle - \langle \Psi_{j,0} | \tau_z | \Psi_{j,0} \rangle = E_{j,1} \langle \Psi_{j,0} | \Psi_{j,0} \rangle. \quad (44)$$

The first term on the left side is zero by virtue of Eq. (42). Then the second term is real, and we have

$$\begin{aligned} \langle \Psi_{j,0} | \tau_z | \Psi_{j,0} \rangle &= \langle \Psi_{j,0} | \tau_z | \Psi_{j,0} \rangle^* = \langle \tilde{\Psi}_{j,0} | \Xi \tau_z | \Psi_{j,0} \rangle \\ &= -\langle \Psi_{j,0} | \tau_z | \Psi_{j,0} \rangle \\ &= 0, \end{aligned} \quad (45)$$

resulting in $E_{j,1} = 0$. Here we used anti-unitarity of Ξ and anticommutation relation $\{\tau_z, \Xi\} = 0$. Eq. (43) with $E_{j,1} = 0$ leads to

$$\mathcal{H}_{\text{BdG}}(0)\Psi_{j,1} = \tau_z \Psi_{j,0}, \quad (46)$$

$$\langle \Psi_{j',0} | \tau_z | \Psi_{j,0} \rangle = 0 \quad \forall j, j' \in \{1, 2\}. \quad (47)$$

If we apply Ξ to Eq. (46)

$$\begin{aligned} \mathcal{H}_{\text{BdG}}(0)\tilde{\Psi}_{j,1} &= \tau_z \tilde{\Psi}_{j,0}, \\ &= \mathcal{H}_{\text{BdG}}(0)\Psi_{j,1}, \end{aligned} \quad (48)$$

allowing us to write

$$\tilde{\Psi}_{j,1} = \Psi_{j,1} + \alpha_{j,1}\Psi_{1,0} + \beta_{j,1}\Psi_{2,0} \quad (49)$$

which will be useful to prove $E_{j,2} = 0$ below, where $\alpha_{j,1}$ and $\beta_{j,1}$ are constants.

We can do the similar procedure as above to get $E_{j,2} = 0$. The μ^2 -order equation with $E_{j,0} = E_{j,1} = 0$ is given by

$$\frac{1}{2!}\mathcal{H}_{\text{BdG}}(0)\Psi_{j,2} - \tau_z \Psi_{j,1} = \frac{1}{2!}E_{j,2}\Psi_{j,0}. \quad (50)$$

Multiplying $\langle \Psi_{j,0} |$ to this equation gives

$$-\langle \Psi_{j,0} | \tau_z | \Psi_{j,1} \rangle = E_{j,2} \langle \Psi_{j,0} | \Psi_{j,0} \rangle. \quad (51)$$

Using Eqs. (47) and (49),

$$\begin{aligned} \langle \Psi_{j,0} | \tau_z | \Psi_{j,1} \rangle &= \langle \Psi_{j,0} | \tau_z | \Psi_{j,1} \rangle^* = -\langle \Psi_{j,0} | \tau_z | \tilde{\Psi}_{j,1} \rangle \\ &= -\langle \Psi_{j,0} | \tau_z | \Psi_{j,1} \rangle - \alpha_{j,1} \langle \Psi_{j,0} | \tau_z | \Psi_{1,0} \rangle - \beta_{j,1} \langle \Psi_{j,0} | \tau_z | \Psi_{2,0} \rangle \\ &= 0, \end{aligned} \quad (52)$$

and we get $E_{j,2} = 0$. From Eq. (50),

$$\frac{1}{2}\mathcal{H}_{\text{BdG}}(0)\Psi_{j,2} = \tau_z\Psi_{j,1} \quad (53)$$

$$\langle\Psi_{j',0}|\tau_z|\Psi_{j,1}\rangle = 0 \quad \forall j, j' \in \{1, 2\}, \quad (54)$$

$$\tilde{\Psi}_{j,2} = \Psi_{j,2} + 2\alpha_{j,1}\Psi_{1,1} + 2\beta_{j,1}\Psi_{2,1} + \alpha_{j,2}\Psi_{1,0} + \beta_{j,2}\Psi_{2,0}, \quad (55)$$

where $\alpha_{j,2}$ and $\beta_{j,2}$ are constants.

We now verify that $E_{j,n} = 0$ for all positive integer n by induction on n . It is assumed that the following conditions from the μ^n -order equation hold:

$$E_{j,k} = 0 \quad \text{for } 0 \leq k \leq n, \quad (56)$$

$$\mathcal{H}_{\text{BdG}}(0)\Psi_{j,n} = n\tau_z\Psi_{j,n-1} \quad (57)$$

$$\langle\Psi_{j',0}|\tau_z|\Psi_{j,k'}\rangle = 0 \quad \forall j, j' \in \{1, 2\}, \text{ and for } 0 \leq k' \leq n-1, \quad (58)$$

$$\tilde{\Psi}_{j,n} = \Psi_{j,n} + \sum_{j'=1,2} \sum_{k'=0}^{n-1} c_{j',k'}\Psi_{j',k'}, \quad (59)$$

where $c_{j',k'}$ are constants. Since we have shown above that these conditions are fulfilled for $n \in \{1, 2\}$, it is enough to show that if they hold for $n = n_0$, then also $n = n_0 + 1$ holds. Using $E_{j,k} = 0$ for $0 \leq k \leq n_0$, the μ^{n_0+1} -order equation is given by

$$\frac{1}{(n_0+1)!}\mathcal{H}_{\text{BdG}}(0)\Psi_{j,n_0+1} - \frac{1}{n_0!}\tau_z\Psi_{j,n_0} = \frac{1}{(n_0+1)!}E_{j,n_0+1}\Psi_{j,0}. \quad (60)$$

If we multiply $\langle\Psi_{j,0}|$ to this equation, we have

$$-\frac{1}{n_0!}\langle\Psi_{j,0}|\tau_z|\Psi_{j,n_0}\rangle = \frac{1}{(n_0+1)!}E_{j,n_0+1}\langle\Psi_{j,0}|\Psi_{j,0}\rangle. \quad (61)$$

Using Eqs. (57) and (58) with $n = n_0$, $\langle\Psi_{j,0}|\tau_z|\Psi_{j,n_0}\rangle$ in the left side can be calculated as

$$\begin{aligned} \langle\Psi_{j,0}|\tau_z|\Psi_{j,n_0}\rangle &= \langle\Psi_{j,0}|\tau_z|\Psi_{j,n_0}\rangle^* = -\langle\Psi_{j,0}|\tau_z|\tilde{\Psi}_{j,n_0}\rangle \\ &= -\langle\Psi_{j,0}|\tau_z|\Psi_{j,n_0}\rangle - \sum_{j'=1,2} \sum_{k'=0}^{n_0-1} c_{j',k'}\langle\Psi_{j,0}|\tau_z|\Psi_{j',k'}\rangle \\ &= 0, \end{aligned} \quad (62)$$

and $E_{j,n_0+1} = 0$. From Eq. (60) we get

$$\mathcal{H}_{\text{BdG}}(0)\Psi_{j,n_0+1} = (n_0+1)\tau_z\Psi_{j,n_0}, \quad (63)$$

$$\langle\Psi_{j',0}|\tau_z|\Psi_{j,n_0}\rangle = 0 \quad \forall j, j' \in \{1, 2\}, \quad (64)$$

$$\tilde{\Psi}_{j,n_0+1} = \Psi_{j,n_0+1} + \sum_{j'=1,2} \sum_{k'=0}^{n_0} c'_{j',k'}\Psi_{j',k'}. \quad (65)$$

Therefore, if Eqs. (56)-(59) hold for $n = n_0$, then they also hold for $n = n_0 + 1$.

C. Time-averaged tunneling current

In this section, we provide the details of the calculation of the time-averaged tunneling current \bar{I} in the main text. It is obtained from the average of $\langle I(t) \rangle$ over a half rotation period,

$$\bar{I} = \frac{1}{T_J} \int_{t_Q - \frac{T_J}{2}}^{t_Q + \frac{T_J}{2}} dt \langle I(t) \rangle, \quad (66)$$

in the limit of very large integer Q so that $t_Q = t_0 + QT_J \gg t_0$. For a time $t \in [t_Q - T_J/2, t_Q + T_J/2]$, $\langle I(t) \rangle$ is roughly proportional to the tip-Majorana tunneling magnitude $\langle I(t) \rangle \propto e^{-\lambda|t-t_Q|}$. Thus $\langle I(t) \rangle$ is maximum when $t = t_Q$, and is exponentially small of the order of $e^{-\lambda T_J/2}$ for $t = t_Q \pm T_J/2$.

We first calculate the tunneling current $\langle I(t) \rangle$ in the time interval $[t_Q - T_J/2, t_Q + T_J/2]$. From Eq. (14) in the main text, we obtain

$$\langle I(t) \rangle = \frac{2e}{\hbar^2} \sum_k \frac{|V_k|^2 \lambda}{\lambda^2 + (\varepsilon_k + eV)^2 / \hbar^2} [-(1 - n_F(\varepsilon_k))A(t, \alpha) + n_F(\varepsilon_k)A(t, -\alpha)], \quad (67)$$

where

$$A(t, \alpha) = e^{2\lambda(t-t_Q)} + e^{\lambda(t-t_Q)} \left\{ \left[\sum_{n=1}^{Q-1} e^{in\alpha} e^{-i(\varepsilon_k + eV)(t-t_{Q-n})/\hbar} \right] + \frac{\lambda + i(\varepsilon_k + eV)/\hbar}{2\lambda} e^{iQ\alpha} e^{-i(\varepsilon_k + eV)(t-t_0)/\hbar} + c.c. \right\} \quad (68)$$

for $t \in [t_Q - T_J/2, t_Q]$, and

$$A(t, \alpha) = -e^{-2\lambda(t-t_Q)} + e^{-\lambda(t-t_Q)} \left\{ \left[\sum_{n=0}^{Q-1} e^{in\alpha} e^{-i(\varepsilon_k + eV)(t-t_{Q-n})/\hbar} \right] + \frac{\lambda + i(\varepsilon_k + eV)/\hbar}{2\lambda} e^{iQ\alpha} e^{-i(\varepsilon_k + eV)(t-t_0)/\hbar} + c.c. \right\} \quad (69)$$

for $t \in [t_Q, t_Q + T_J/2]$. $A(t, -\alpha)$ is obtained by replacing α by $-\alpha$ from $A(t, \alpha)$. In this calculation, we neglected the terms of the order of $e^{-\lambda T_J/2}$ that give an exponentially small contribution to $A(t, \alpha)$ in our limit of the short duration of the tunneling $\lambda^{-1} \ll T_J$. Then \bar{I} can be expressed as

$$\bar{I} = \frac{2e}{\hbar^2} \sum_k \frac{|V_k|^2 \lambda}{\lambda^2 + (\varepsilon_k + eV)^2 / \hbar^2} \left\{ -(1 - n_F(\varepsilon_k)) \left[\frac{1}{T_J} \int_{t_Q - T_J/2}^{t_Q + T_J/2} dt A(t, \alpha) \right] + n_F(\varepsilon_k) \left[\frac{1}{T_J} \int_{t_Q - T_J/2}^{t_Q + T_J/2} dt A(t, -\alpha) \right] \right\}, \quad (70)$$

To calculate \bar{I} we have to calculate the time averages of $A(t, \alpha)$ and $A(t, -\alpha)$. It is given by

$$\begin{aligned} \frac{1}{T_J} \int_{t_Q - T_J/2}^{t_Q + T_J/2} dt A(t, \alpha) &= \frac{1}{T_J} \left\{ \frac{2\lambda}{\lambda^2 + (\varepsilon_k + eV)^2 / \hbar^2} \left[\sum_{n=-Q}^Q e^{in\alpha} e^{-i(\varepsilon_k + eV)nT_J/\hbar} \right] \right. \\ &\quad \left. + \left[\frac{-\lambda + i(\varepsilon_k + eV)/\hbar}{\lambda^2 + (\varepsilon_k + eV)^2 / \hbar^2} e^{i\alpha Q} e^{-i(\varepsilon_k + eV)QT_J/\hbar} + c.c. \right] \right\}. \end{aligned} \quad (71)$$

In the limit that Q goes to infinity, the summation term over n on the right side can be written as

$$\begin{aligned} \lim_{Q \rightarrow \infty} \sum_{n=-Q}^Q e^{in\alpha} e^{-i(\varepsilon_k + eV)nT_J/\hbar} &= 2\pi \sum_{l=-\infty}^{\infty} \delta \left[\alpha - \frac{(\varepsilon_k + eV)T_J}{\hbar} - 2\pi l \right] \\ &= \frac{2\pi\hbar}{T_J} \sum_{l=-\infty}^{\infty} \delta \left[-\varepsilon_k - eV + \frac{(\alpha - 2\pi l)\hbar}{T_J} \right], \end{aligned} \quad (72)$$

where $l = 0, \pm 1, \pm 2, \dots$, while the remaining terms that possess $e^{\pm i\varepsilon_k QT_J/\hbar}$ factors can be neglected because of their rapid oscillation as a function of k for large Q

$$\sum_k e^{\pm i\varepsilon_k QT_J/\hbar} \sim 0. \quad (73)$$

Thus the time averages of $A(t, \alpha)$ and $A(t, -\alpha)$ (obtained by replacing α by $-\alpha$ in $A(t, \alpha)$) have the forms

$$\begin{aligned} \frac{1}{T_J} \int_{t_Q - \frac{T_J}{2}}^{t_Q + \frac{T_J}{2}} dt A(t, \alpha) &= \frac{2\lambda}{\lambda^2 + (\varepsilon_k + eV)^2/\hbar^2} \frac{2\pi\hbar}{T_J^2} \sum_{l=-\infty}^{\infty} \delta \left[-\varepsilon_k - eV + \frac{(\alpha - 2\pi l)\hbar}{T_J} \right], \\ \frac{1}{T_J} \int_{t_Q - \frac{T_J}{2}}^{t_Q + \frac{T_J}{2}} dt A(t, -\alpha) &= \frac{2\lambda}{\lambda^2 + (\varepsilon_k + eV)^2/\hbar^2} \frac{2\pi\hbar}{T_J^2} \sum_{l'=-\infty}^{\infty} \delta \left[-\varepsilon_k - eV - \frac{(\alpha + 2\pi l')\hbar}{T_J} \right], \\ &= \frac{2\lambda}{\lambda^2 + (\varepsilon_k + eV)^2/\hbar^2} \frac{2\pi\hbar}{T_J^2} \sum_{l'=-\infty}^{\infty} \delta \left[-\varepsilon_k - eV - \frac{(\alpha - 2\pi l')\hbar}{T_J} \right]. \end{aligned} \quad (74)$$

In the last line of the second equation, we changed l' by $-l'$ for convenience. If we put these into Eq. (70), it follows that

$$\begin{aligned} \bar{I} = \frac{e}{\hbar^2} \sum_k |V_k|^2 \frac{2\pi\hbar}{T_J^2} \left[\frac{2\lambda}{\lambda^2 + (\varepsilon_k + eV)^2/\hbar^2} \right]^2 &\left\{ - (1 - n_F(\varepsilon_k)) \sum_{l=-\infty}^{\infty} \delta \left[-\varepsilon_k - eV + \frac{(\alpha - 2\pi l)\hbar}{T_J} \right] \right. \\ &\left. + n_F(\varepsilon_k) \sum_{l'=-\infty}^{\infty} \delta \left[-\varepsilon_k - eV - \frac{(\alpha - 2\pi l')\hbar}{T_J} \right] \right\}. \end{aligned} \quad (75)$$

By replacing the discrete sum over k by an integral with the density of states of the metallic tip $\rho(\varepsilon_k)$

$$\sum_k \rightarrow \int d\varepsilon_k \rho(\varepsilon_k). \quad (76)$$

Assuming a wide-band limit with an energy independent tunneling rate $\Gamma = 2\pi\rho(\varepsilon_k)|V_k|^2$, we obtain

$$\begin{aligned} \bar{I} &= \frac{e}{\hbar} \sum_l 2\pi\Gamma \left[\frac{2\lambda T_J}{\lambda^2 T_J^2 + (\alpha - 2\pi l)^2} \right]^2 [-n_F(eV - (\alpha - 2\pi l)\hbar/T_J) + n_F(-eV - (\alpha - 2\pi l)\hbar/T_J)] \\ &= \frac{e}{\hbar} \sum_l Z_l(\alpha) [-n_F(V_l^+(\alpha)) + n_F(V_l^-(\alpha))], \end{aligned} \quad (77)$$

where $Z_l(\alpha)$ and $V_l^\pm(\alpha)$ are defined in the main text. It is now straightforward to evaluate the time-averaged differential conductance $d\bar{I}/dV$. Since only the Fermi-Dirac distributions have the voltage dependence, it is enough to compute

$$\begin{aligned} \frac{dn_F(V_l^\pm(\alpha))}{dV} &= \frac{d}{dV} \frac{1}{1 + \exp[V_l^\pm(\alpha)/(k_B T)]} \\ &= \mp \frac{e}{4k_B T} \operatorname{sech}^2[V_l^\pm(\alpha)/(2k_B T)]. \end{aligned} \quad (78)$$

Therefore, we get

$$\frac{d\bar{I}}{dV} = \frac{e^2}{\hbar} \sum_l \frac{Z_l(\alpha)}{4k_B T} \left\{ \operatorname{sech}^2 \left[\frac{V_l^+(\alpha)}{2k_B T} \right] + \operatorname{sech}^2 \left[\frac{V_l^-(\alpha)}{2k_B T} \right] \right\}. \quad (79)$$

D. Floquet description of the two rotating Majorana bound states

In the previous section, we showed that the time-averaged differential conductance has peaks at $eV = \pm(\alpha - 2\pi l)\hbar/T_J$. Here, we provide an alternative derivation of the result by considering an effective Floquet Hamiltonian for the two rotating Majorana bound states in our Corbino-geometry Josephson junction. The Floquet description is valid as the time-dependent BdG Hamiltonian in Eq.(7) in the main text is periodic in time with period T_J : $H_{\text{BdG}}[\Delta\phi(t')] = H_{\text{BdG}}[\Delta\phi(t' + T_J)]$ where $\Delta\phi$ is the phase difference across the junction. The time evolution operator

of the Hamiltonian from t' to $t' + T_J$ in our low-energy subspace is U_M in Eq. (17) in the main text, and the effective Floquet Hamiltonian H_F [S2] is obtained by using

$$e^{-iH_F T_J/\hbar} = U_M, \quad (80)$$

which yields

$$H_F = i\frac{\varepsilon}{2}\gamma_2(t_0)\gamma_1(t_0) + 2\pi l\frac{\hbar}{T_J}, \quad (81)$$

where $\varepsilon = \alpha\hbar/T_J$ and integer l . The first term is reminiscent to the Hamiltonian for two coupled static MBS with hybridisation ε (which shows conductance peaks at $eV = \pm\varepsilon$), and the second term shifts energy levels. As a result, tunneling into an effective system described by H_F gives conductance peaks at $eV = \pm\varepsilon + 2\pi l\hbar/T_J$ which is producing our features above.

E. Weak disorder effect

In this section, we show that two Majorana bound states in a Corbino-geometry Josephson junction are robust against weak disorder on the surface of a topological insulator if we stay in the subspace spanned by the two Majorana bound states, i.e., they remain at zero energy. It can be shown by using a Taylor expansion in the same way as in Section B. The surface of a topological insulator with a disorder potential is described by

$$H = v_F\vec{\sigma} \cdot \vec{p} + V(\vec{r}), \quad (82)$$

where $V(\vec{r})$ is the disorder potential. Then the BdG equation is given by

$$\left[\begin{pmatrix} v_F\vec{\sigma} \cdot \vec{p} & \Delta(r, \theta)\mathbb{I} \\ \Delta^*(r, \theta)\mathbb{I} & -v_F\vec{\sigma} \cdot \vec{p} \end{pmatrix} + \begin{pmatrix} \lambda V(\vec{r}) & 0 \\ 0 & -\lambda V(\vec{r}) \end{pmatrix} \right] \Psi'_j(r, \theta) = E'_j \Psi'_j(r, \theta). \quad (83)$$

Here a perturbation parameter λ is introduced to keep track of the order of the disorder potential in a Taylor expansion, and $\Psi'_{j=1,2}(r, \theta)$ and E'_j are eigenfunctions and eigenvalues, respectively, which are assumed to be differentiable functions with respect to λ . Like in the case of the calculation in Section B, we do a Taylor expansion for $\Psi'_{j=1,2}(r, \theta)$ and E'_j in λ ,

$$E'_j = E'_{j,0} + \lambda E'_{j,1} + \frac{\lambda^2}{2!} E'_{j,2} + \frac{\lambda^3}{3!} E'_{j,3} + \dots, \quad (84)$$

$$\Psi'_j = \Psi'_{j,0} + \lambda \Psi'_{j,1} + \frac{\lambda^2}{2!} \Psi'_{j,2} + \frac{\lambda^3}{3!} \Psi'_{j,3} + \dots \quad (85)$$

Now we substitute these expansions into the BdG equation and equate terms of the same order in λ . All calculation details are the same as in Section B, except that μ and $-\tau_z$ in Section B are replaced by λ and $V(\vec{r})\tau_z$ where τ_z is the Pauli matrix in particle-hole space, and we get

$$E'_{j,k} = 0, \quad (86)$$

for all $j \in \{1, 2\}$ and nonnegative integer k . Therefore we conclude that two Majorana bound states are robust against a weak disorder potential, and hence the results shown in Fig. 3 in the main text can be detected even in the presence of weak disorder.

[S1] L. Fu and C. L. Kane, Phys. Rev. Lett **100**, 096407 (2008).

[S2] J. Cayssol, B. Dóra, F. Simon, and R. Moessner, Phys. Status Solidi RRL **7**, 101 (2013).